J Solid State Electrochem (2011) 15:1977–1985
DOI 10.1007/s10008-010-1220-8

ORIGINAL PAPER

Effects of current densities on the formation of $LiCoO_2$/graphite lithium ion battery

Yan-Bing He · Baohua Li · Quan-Hong Yang · Hongda Du · Feiyu Kang · Guo-Wei Ling · Zhi-Yuan Tang

Received: 16 January 2010 / Revised: 5 October 2010 / Accepted: 10 October 2010 / Published online: 27 October 2010

Abstract The activation characteristics and the effects of current densities on the formation of a separate $LiCoO_2$ and graphite electrode were investigated and the behavior also was compared with that of the full $LiCoO_2$/graphite batteries using various electrochemical techniques. The results showed that the formation current densities obviously influenced the electrochemical impedance spectrum of Li/graphite, $LiCoO_2$/Li, and $LiCoO_2$/graphite cells. The electrolyte was reduced on the surface of graphite anode between 2.5 and 3.6 V to form a preliminary solid electrolyte interphase (SEI) film of anode during the formation of the $LiCoO_2$/graphite batteries. The electrolyte was oxidized from 3.95 V vs Li^+/Li on the surface of $LiCoO_2$ to form a SEI film of cathode. A highly conducting SEI film could be formed gradually on the surface of graphite anode, whereas the SEI film of $LiCoO_2$ cathode had high resistance. The $LiCoO_2$ cathode could be activated completely at the first cycle, while the activation of the graphite anode needed several cycles. The columbic efficiency of the first cycle increased, but that of the second decreased with the increase in the formation current of $LiCoO_2$/graphite batteries. The formation current influenced the cycling performance of batteries, especially the high-temperature cycling performance. Therefore, the batteries should be activated with proper current densities to ensure an excellent formation of SEI film on the anode surface.

Keywords $LiCoO_2$/graphite batteries · Formation current · Solid electrolyte interphase (SEI) film · Columbic efficiency (CE) · Cycling performance

Y.-B. He · B. Li · Q.-H. Yang · H. Du · F. Kang (✉)
Advanced Materials Institute, Graduate School at Shenzhen,
Tsinghua University,
Shenzhen 518055, China
e-mail: fykang@mail.tsinghua.edu.cn

Q.-H. Yang · G.-W. Ling · Z.-Y. Tang
Department of Applied Chemistry, School of Chemical
Engineering and Technology, Tianjin University,
Tianjin 300072, China

Introduction

The electrolyte is reduced on the surface of anode or oxidized on the surface of cathode to form a surface film called the solid electrolyte interphase (SEI) during first charge and discharge of lithium ion batteries [1–5]. In the case of graphite anode, the SEI layer plays an important role for lithium intercalation/de-intercalation. The formation of a stable SEI can inhibit the further decomposition of electrolyte on the negative electrode and stabilize the negative electrode. The life, discharge, and safety performance of lithium ion batteries are highly dependent on the SEI film of carbon electrode. The structure of an excellent SEI film is stable and compact, which cannot be destroyed easily at high temperature; thus, the reaction of lithiated carbon anode with electrolyte will reduce greatly [6]. The SEI layer is usually formed during the first cycle and stably remained on the surface during intercalation/de-intercalation processes continuing in further cycles [7]. An irreversible electrolyte reduction decomposition would further proceed if the SEI layer on the anode is not thick enough to prevent electron tunneling through it. Therefore, a stable SEI layer is required for the carbonaceous electrode,

which is electronically insulating but conducting to lithium ions [8, 9]. Thus, before being placed on the market, lithium ion batteries must undergo one or more charge–discharge cycles, which is conventionally called the formation process, to make sure that the SEI layer has been fully grown [5, 8, 9]. However, in the case of $LiCoO_2$, a very thin SEI film is formed on the active material but not on the binders during first charge, and the surface film is not so stable and strips off during the discharge process due to the weak interaction between the surface film and $LiCoO_2$ electrode surface [7, 10]. At present, the function and effects of the SEI film of the cathode on the performance of batteries is ambiguous.

The performance of the SEI film and cells is affected by various formation factors (e.g., the formation charge–discharge current, cutoff voltage, formation temperature, solvent and lithium salt, carbon electrode, and so on) [5, 8, 9, 11–13]. The cycling performance of $LiCoO_2$/graphite batteries at high temperature becomes worse with the increase in the formation temperature [12]. The optimum cutoff voltage is not <3.7 V for industrial $LiCoO_2$/graphite batteries [5]. The SEI film composition and morphology is affected by the carbon substrate and electrolyte salt [13]. However, there are no studies about the effects of current densities on the formation of commercial $LiCoO_2$/graphite batteries. Hence, in this paper, we attempted to investigate the activation characteristics and the effects of current densities on the formation of a separate $LiCoO_2$ and graphite electrode and compared the behavior with that of the full $LiCoO_2$/graphite using various electrochemical techniques, especially the electrochemical impedance spectroscopy technique, which is a very powerful tool to analyze the electrode reactions and formation of the SEI film.

Experimental

Commercial 041428-type lithium ion batteries, which are nominally 4 mm thick, 14 mm wide, and 28 mm long, were assembled to investigate the effects of current densities on the formation of $LiCoO_2$/graphite batteries. The nominal capacity of the batteries was designed to be 120 mAh. The batteries were assembled with $LiCoO_2$ (Tianjin B&M Science and Technology Joint-Stock Co., Ltd, China) as cathodes, graphite as anodes, and polyethylene as separator. The $LiCoO_2$ cathodes consisted of 90 wt.% $LiCoO_2$, 5 wt.% conductive carbon black, and 5 wt.% poly (vinylidene fluoride). The graphite anodes consisted of 91 wt.% composite graphite, 6 wt.% styrene–butadiene rubber, and 3 wt.% carboxymethyl cellulose. $LiPF_6$ (1 M) in a 1:1:1 mixture of ethylene carbonate/dimethyl carbonate/ethylene methyl carbonate (1 M $LiPF_6$/EC+DMC+EMC) was used as the standard electrolyte. The negative electrode, positive electrode, and separator were rolled together to make the battery core, and then the core was put into 041428-type aluminum plastic-laminated film box. The electrolyte was injected and the batteries were sealed with a sealing machine. Some 2032-type Li/graphite and $LiCoO_2$/Li coin half cells were also assembled using the graphite electrode, $LiCoO_2$ electrode, polyethylene separator, electrolyte, and lithium foil. The cell assembly was conducted in an argon-filled glove box.

The 2032-type Li/graphite half cells were charged and discharged five times with different current densities of 15, 30, 60, 150, and 300 mA/g using a Land 2001A cell test system, and the $LiCoO_2$/Li half cells also were charged and discharged five times with different current densities of 7, 14, 28, 70, and 140 mA/g. The electrochemical working station (Gamry Instrument model PCI 4-750) was used to measure the cyclic voltammograms (CV) and electrochemical impedance spectrum (EIS) of cells. EIS of the Li/graphite half cells were measured at the voltage of 0.06 V with graphite electrode as the working electrode and one piece of lithium electrode as both the reference and counter electrodes. Meanwhile, EIS of $LiCoO_2$/Li half cells were also tested at the voltage of 4.2 V with $LiCoO_2$ electrode as the working electrode and lithium electrode as both the reference and counter electrodes. The impedance was measured by applying 5 mV of ac oscillation with the frequency ranging from 100 kHz to 0.01 Hz. CV of the 2032-type Li/graphite and $LiCoO_2$/Li half cells were performed with graphite and $LiCoO_2$ electrodes as the working electrodes and lithium electrode as both the reference and counter electrodes. A scanning rate of 0.05 mV/s was applied with a sweep voltage range of 2.0–0.0 V for Li/graphite half cells and 3.2–4.4 V for $LiCoO_2$/Li half cells, respectively.

The formation and cycling performance tests of the 041428-type $LiCoO_2$/graphite batteries were performed using the BS-9300 lithium ion battery tester. Multistage constant current–constant voltage first charging protocols were designed to study the effects of current on the formation of $LiCoO_2$/graphite batteries. In all protocols, a constant voltage charging was applied to achieve the fully charged state after the cell voltage reached 4.2 V until the current declined to 0.01 C. Then, the batteries were discharged at a constant current of 60 mA (0.5 C) to a cutoff voltage of 2.75 V. The formation protocols were listed in Table 1. EIS of the 041428-type $LiCoO_2$/graphite batteries at 3.95 V and CV of the batteries before formation were tested with $LiCoO_2$ electrodes as the working electrodes and graphite electrodes as both the reference and counter electrodes. The cycling performance of batteries with different formation currents was tested between 2.75 and 4.2 V using a current of 60 mA (0.5 C) at 25 and 50 °C, respectively.

Table 1 Formation protocols of 041428-type $LiCoO_2$/graphite batteries

Number	Formation protocols
a	0.05 C charge to 3.0 V, 0.1 C to 4.2 V, 0.5 C discharge
b	0.05 C charge to 3.0 V, 0.1 C to 3.85 V, 0.2 C to 4.2 V, 0.5 C discharge
c	0.2 C charge to 4.2 V, 0.5 C discharge
d	0.3 C charge to 4.2 V, 0.5 C discharge

Results and discussion

The first charge and discharge curves of Li/graphite and $LiCoO_2$/Li half cells with different formation current densities are given in Fig. 1a, b. It can be found that the lithiation potential of graphite and $LiCoO_2$ electrodes decreases and the delithiation potential increases with the increase in the formation current density. The discharge curves of graphite anodes show typical three-order lithiation plateaus at the voltage of 0.2, 0.08, and 0.06 V, respectively. EIS of the Li/graphite and $LiCoO_2$/Li half cells after five cycles are plotted in Fig. 1c, d. All cells were cycled five times before the EIS measurement to ensure a complete formation of the SEI on the graphite anodes and complete activation of the $LiCoO_2$ cathodes. As shown in Fig. 2a, b, the EIS of Fig. 1c, d were simulated by Z-view software using the equivalent circuit of Fig. 2c. Values of impedance parameters were listed in Tables 2 and 3. It can be observed that the experimental and simulation EIS are almost coincident, which indicates that the EIS of graphite and $LiCoO_2$ electrodes fit the same equivalent circuit. According to the equivalent circuit, the EIS of Li/graphite and $LiCoO_2$/Li cells are composed of two partially overlapped and depressed semicircles at high to middle frequency and a slope line at low frequency [14–17]. The intersection of the diagram with real axis refers to a bulk resistance (R_b), which reflects the electronic and ionic resistance of two electrodes and electrolyte/separator. CPE1

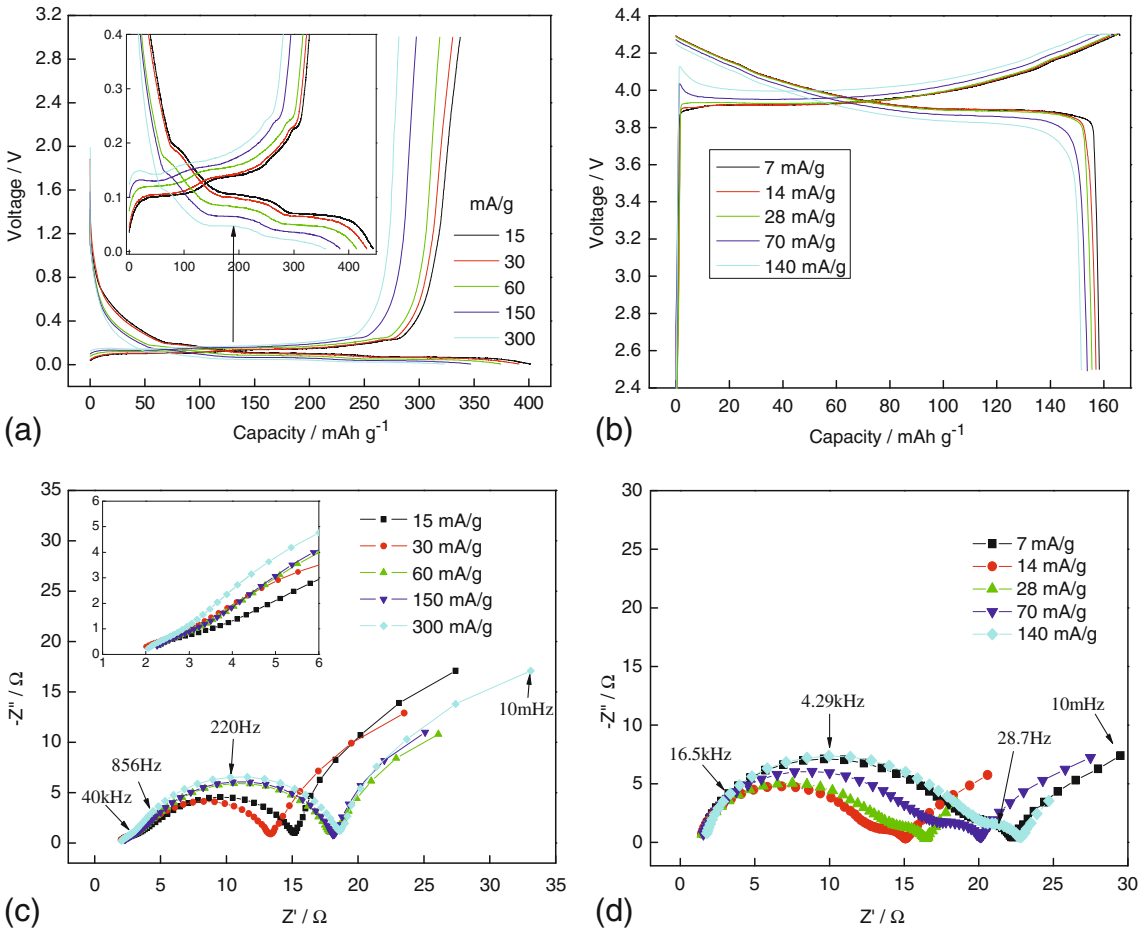

Fig. 1 First charge and discharge curves of Li/graphite and $LiCoO_2$/Li half cells (**a**, **b**) with different current density and EIS of Li/graphite and $LiCoO_2$/Li half cells (**c**, **d**) after five cycles with different current densities

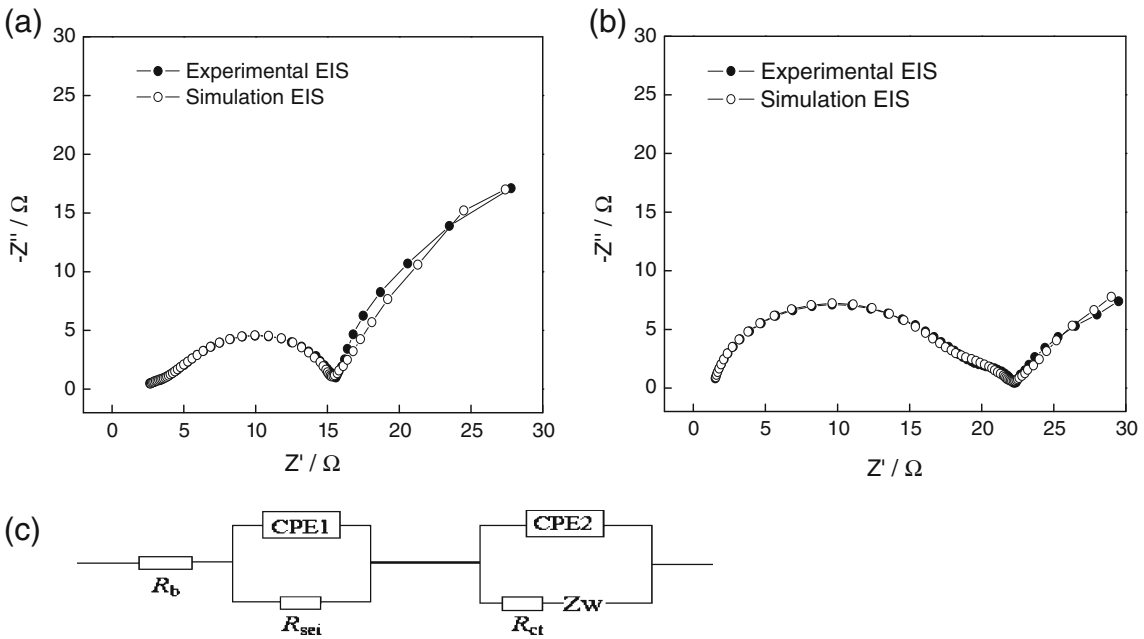

Fig. 2 Experimental and simulation EIS curves of Li/graphite half cells after five cycles at a current density of 15 mAh/g (**a**) and $LiCoO_2$/Li half cells after five cycles at a current density of 7 mAh/g (**b**) using the equivalent circuit (**c**) by Z-view software

and CPE2 are the constant phase elements which were used instead of capacitance (C_{sei}) of the solid electrolyte and double-layer capacitance (C_{dl}), respectively, to take into account the roughness of the particle surface. The depressed semicircle at high frequency could be attributed to the resistance (R_{sei}) and CPE1. The depressed semicircle at medium frequency could be attributed to the charge transfer resistance (R_{ct}) and CPE2. The slope line at low frequency corresponds to the Warburg impedance (Z_w), which is related to the lithium ion diffusion within the particles[16].

It can be found in Table 2 that the R_{ct} of Li/graphite cells is obviously larger than the R_{sei}, which may be attributed to the high lithium ion conductivity of the SEI film on the surface of graphite. It is interesting to note that the R_{sei} decreases with the increase of the formation current. This observation can be explained in terms of the morphology of the SEI film. It is well known that during the first charge and discharge of batteries, the electrolyte is reduced to form a surface film called SEI on the graphite anode and the SEI film is electronically insulating but conducting to lithium ions [3, 9, 11, 12]. The ionic conductivity of the SEI film depends on two factors: one is the morphology of the SEI film and the other is the property of the liquid electrolyte. For the studied half cells, the liquid electrolyte is 1 M $LiPF_6$/EC+DMC+EMC and each cell contains the same quantity of electrolyte, which indicates that the liquid electrolyte almost does not influence the discussion of the ionic conductivity of the SEI film. Thus, the morphology of the SEI film may be the main factor influencing the ionic conductivity of the SEI film. In fact, when a higher current density is applied to the first charge and discharge, the resulting SEI is more loose (or porous) and less adhesive, which makes the lithium ion pass through the SEI film more easily. Of course, the SEI with loose structure may not be sufficiently denser to prevent further electron tunneling. Therefore, the SEI formed with higher formation

Table 2 Impedance parameters of Fig.1c calculated using the equivalent circuit of Fig. 2c (the unit of *R* and CPE-*T* are Ω/cm^2 and F/cm^2, respectively)

Current density (mA/g)	*R*b	*R*sei	*R*ct	CPE1		CPE2		*Z*w		
				T	P	*T*×E-5	P	*R*	*T*	*P*
15	3.20	5.07	14.63	0.000698	0.526	9.75	0.908	84.06	12.30	0.692
30	2.57	4.22	12.96	0.000982	0.539	10.68	0.915	65.72	13.18	0.665
60	2.99	4.26	19.41	0.000577	0.576	7.61	0.910	55.08	13.34	0.659
150	2.97	4.25	19.68	0.000541	0.584	7.05	0.923	53.96	13.42	0.706
300	2.82	3.15	21.38	0.000506	0.616	6.33	0.926	88.22	11.84	0.673

Table 3 Impedance parameters of Fig.1d calculated using the equivalent circuit of Fig. 2c (the unit of *R* and CPE-*T* are Ω/cm^2 and F/cm^2, respectively)

Current density (mA/g)	*R*b	*R*sei	*R*ct	CPE1		CPE2		*Z*w		
				T×E−6	*P*	*T*	*P*	*R*	*T*	*P*
7	2.13	23.21	7.88	3.57	0.918	0.00083	0.715	40.67	72.87	0.573
14	2.12	15.26	5.28	2.71	0.943	0.00171	0.676	31.34	73.76	0.579
28	2.25	16.08	6.66	3.71	0.925	0.00136	0.657	38.60	73.88	0.584
70	2.10	19.85	7.97	3.73	0.923	0.00145	0.679	40.88	74.17	0.578
140	2.55	23.48	8.28	3.12	0.934	0.00151	0.643	38.19	76.53	0.597

current density has relatively higher ionic and electronic conductivity [9], which results in the less value of the R_{sei}. It also can be found that the R_{ct} decreases with the formation current density increasing from 15 to 30 mA/g, increases greatly from 30 to 60 mA/g, and increases smoothly from 60 to 300 mA/g. Therefore, the R_{ct} is least when the formation current density is 30 mA/g.

Z_w is the Warburg impedance due to the lithium ion diffusion within the particle and can be expressed as follows:

$$Z_w = \frac{R \times ctnh((j\omega T)^P)}{(j\omega T)^P}$$

where R is diffusion resistance, $T = L^2/D$ (L is the effective diffusion thickness and D is the effective diffusion coefficient of the particle), $0<P\leq 1$. The values of R, T, and P were listed in Table 2. It can be concluded that the diffusion coefficient of lithium ion within the lithiated graphite particles decreases slightly from 15 to 150 mA/g and increases from 150 to 300 mA/g.

For the $LiCoO_2$/Li cells with different formation current densities, it can be seen in Table 3 that the R_{sei} is obviously larger than the R_{ct}. This result is opposite to that of the Li/graphite cells. It is well known that the resistivity of the $LiCoO_2$ as lithium-containing transitional metal oxides is much higher than that of the graphite. A very thin SEI film also is formed on the surface of the $LiCoO_2$ electrode during formation, and the R_{sei} decreases to a constant value during the first charge [18, 19]. The SEI film on the cathode is thinner than that of the negative electrode and is not so stable and strips off during the discharge process due to the weak interaction between the surface film and $LiCoO_2$ electrode surface [7, 10]. Therefore, a highly conducting SEI film is not formed on the surface of the $LiCoO_2$ electrode, whereas it can be formed on the surface of the graphite electrode. This leads to the much larger R_{sei} of the $LiCoO_2$ electrode than that of the graphite electrode. The R_{sei} and R_{ct} also change with an increase in the formation current density, which decrease in the beginning and then increase with the increase in the formation current. In addition, it can be concluded that the diffusion coefficient of lithium ion within the delithiated $LiCoO_2$ particles decreases slightly with the increase of the formation current density. Tables 2 and 3 also show that the R_{ct} of $LiCoO_2$ electrode is much less than that of the graphite electrode. Therefore, the charge and discharge reaction of $LiCoO_2$/graphite batteries may be controlled by the lithiation and delithiation reactions of the graphite anode.

The CVs of Li/graphite and $LiCoO_2$/Li half cells were tested with a scanning rate of 0.05 mV/s to investigate the formation characteristics of the graphite and $LiCoO_2$ electrodes (see Fig. 3). It can be seen in Fig. 3a that the reduction current in the first cycle increases at 1.0 V and shows a reduction peak at 0.8 V. This is due to the well-known electroreductive formation of SEI film on the graphite anode. The current increases again at 0.2 V, which is attributed to the lithiation reaction of the graphite anode. However, the first to fifth CVs show different characteristics below 0.2 V. The current increases gradually between 0.2 and 0.0 V in the first CV and there is not an obvious lithiation peak, whereas two lithiation peaks at ~0.2 and 0.07 V can be observed from the second to fifth CVs between 0.2 and 0.0 V, which corresponds to the three-order lithiation plateau. The lithiation peaks at 0.08 and 0.06 V overlap and the lithiation peak at 0.07 V only can be observed.

It is interesting to note that the lithiation current peak at 0.2 V almost does not change from the second to fifth CVs, while the peak current of 0.07 V increases. In addition, the delithiation peak current increases with the increase in CV times. Therefore, it can be obtained that the graphite anode is activated gradually during CVs. These phenomena may be attributed to the formation of SEI film on the graphite anode. Zhang et al. [11] reported that a preliminary SEI film was formed on the anode surface above 0.15 V and a highly conductive SEI was formed from 0.15 to 0.04 V during the first charge and discharge. In fact, from the results of current change of Fig. 3a, it can be obtained that the highly conductive SEI may be formed gradually from 0.15 to 0.04 V and the R_{sei} decreases during CVs. Thus, it is

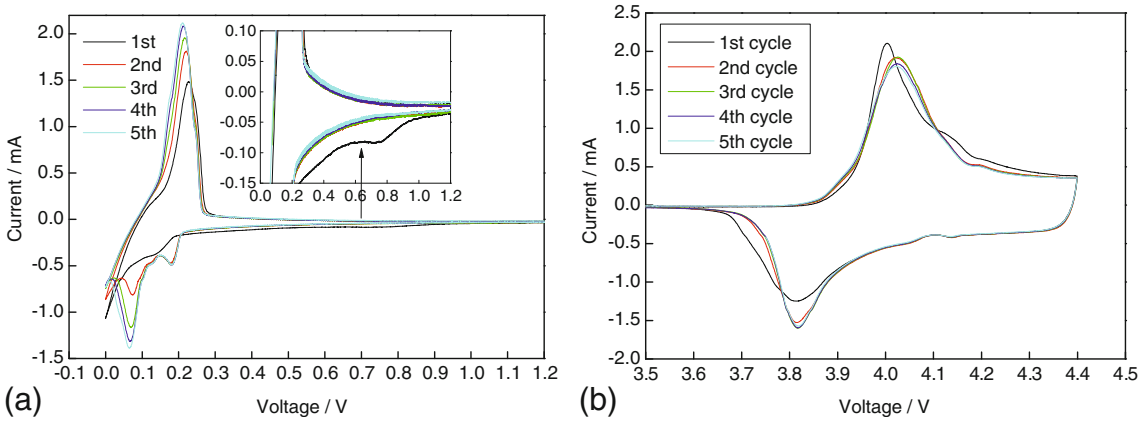

Fig. 3 CV of Li/graphite (**a**) and $LiCoO_2$/Li (**b**) half cells with a scanning rate of 0.05 mV/s

easier for lithium ion to go through the SEI film, which results in the increase of lithiation peak current from the second to fifth CVs. For the CVs of $LiCoO_2$/Li half cells, the oxidation current in the first CV is larger from 3.95 V compared with that of the second to fifth CVs (see Fig. 3b), which indicates that electrolyte is oxidized from 3.95 V on the $LiCoO_2$ cathode surface and a SEI film is formed. The overlapping of the second to fifth CV curves means that the $LiCoO_2$ cathode can be activated in the first cycle, which is quite different from that of the graphite anode.

The CV of 041428-type $LiCoO_2$/graphite batteries before formation was examined to compare the CV behavior with that of the separate graphite and $LiCoO_2$ electrode during formation. It is seen in Fig. 4 that the current in the first CV of 2.5–3.6 V is larger than that of the second to fourth CVs, while the current of the second to fourth CVs between 2.5 and 3.6 V is almost same. The first CV of $LiCoO_2$/Li half cells indicates that there is no obvious reaction below 3.85 V (see Fig. 3b). Thus, the larger current in the first CV of $LiCoO_2$/graphite batteries from 2.5 to 3.6 V can be attributed to the electrolyte reduction on the surface of graphite anode to form a preliminary SEI film during the formation of $LiCoO_2$/graphite batteries. The cathodic polarization current increases quickly from 3.7 V, which indicates that the delithiation of $LiCoO_2$ cathode and lithiation of graphite anode occurs at 3.7 V for $LiCoO_2$/graphite batteries. It is interesting to note that the polarization of the first CV is obviously larger than that of the second to fourth CVs. This phenomenon appears at the lithiation process of 0.2–0.0 V of the graphite anode (see Fig. 3a), whereas it does not appear at the delithiation process of the $LiCoO_2$ cathode (see Fig. 3b). Therefore, the larger polarization of the first CV for $LiCoO_2$/graphite batteries is attributed to the graphite anode. Figure 4 also shows that there are two cathodic polarization peaks on the second to fourth CVs at ~3.8 and 4.1 V, respectively, and the peak current increases but the peak voltage decreases with the increase in the CV times. As we have known from Fig. 3a, the second to fifth CVs for Li/graphite half cells have two lithiation peaks at ~0.2 and 0.07 V, respectively, while the CV of $LiCoO_2$/Li cells only contains a delithiation peak(see Fig. 3b). Thus, the two cathodic polarization peaks of $LiCoO_2$/graphite batteries result from the lithiation of graphite anode. A highly conducting SEI film of graphite anode for $LiCoO_2$/graphite batteries could be formed above 3.7 V.

The formation of the 041428-type $LiCoO_2$/graphite batteries were performed using the formation protocols of Table 1. It can be seen in Fig. 5a that the voltage of batteries increases gradually from 2.4 to 3.7 V using the formation protocols of a and b. The consumption capacity is 14.5 mAh. However, the voltage of batteries increases from 3.1 to 3.7 V using the formation protocols of c and d; the consumption capacity is 10.4 and 9.6 mAh, respectively. As we have known from Fig. 4, a preliminary SEI film was formed on the anode surface of $LiCoO_2$/graphite batteries between 2.5 and 3.6 V. Therefore, the consumption capacity among this voltage region is mainly used for the SEI film formation. The coulombic efficiency (CE) was

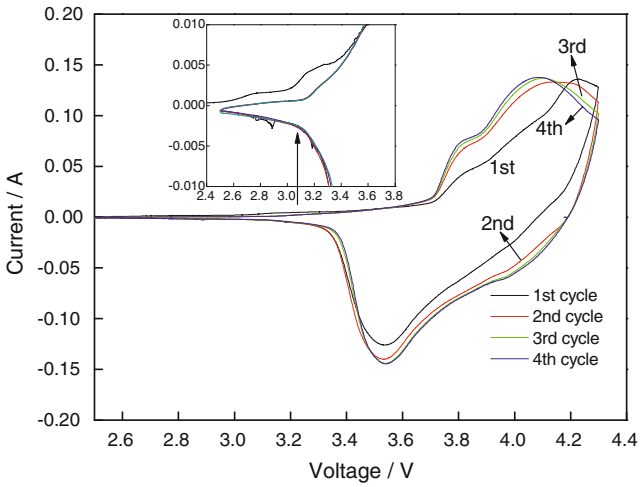

Fig. 4 CV of 041428-type $LiCoO_2$/graphite batteries before formation

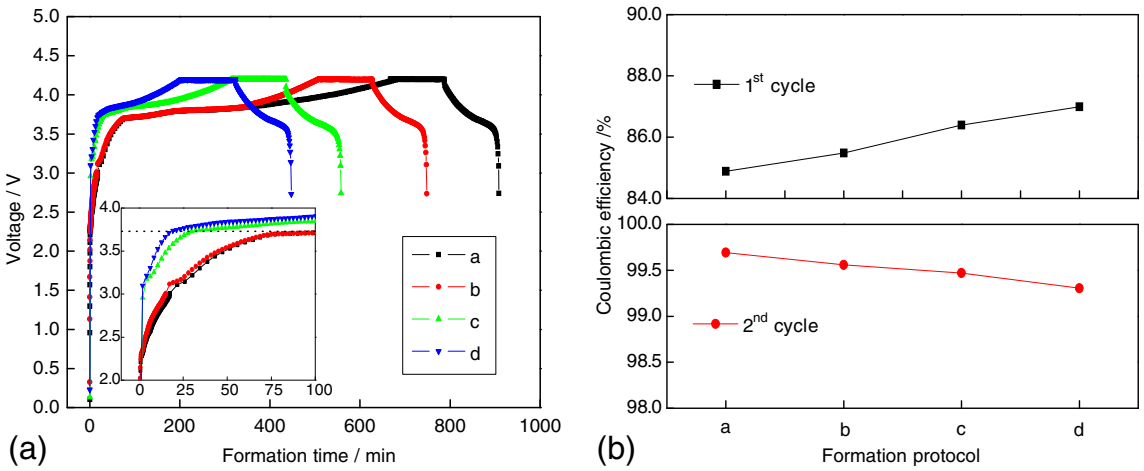

Fig. 5 First charge and discharge curves of 041428-type batteries (**a**) and CE of the first and second charge and discharge (**b**)

investigated during the first and second charge and discharge of $LiCoO_2$/graphite batteries. As shown in Fig. 5b, the CE of the first cycle increases, while that of the second cycle decreases with the increase in the formation current. The voltage of batteries increases quickly using a big formation current due to the larger polarization (see Fig. 5a). There is not enough time to form a good SEI film. The irreversible reaction for the formation of SEI film between 2.5 and 3.6 V is not sufficient, which results in the SEI film having a loose texture and poor adhesion to the surface of graphite [9]. Such a SEI film cannot protect well the electrolytic solvents from further reduction. Thus, the CE of second cycle decreases with the increase of the formation current. Whereas the voltage of batteries with little formation current increases gradually from 2.4 to 3.7 V, there is enough time for the nucleation and growth of the SEI film. A stable and excellent SEI film is formed on the graphite anode. Therefore, the CE of the first cycle decreases with the decrease in the formation current.

The EIS of the 041428-type $LiCoO_2$/graphite batteries also was tested to compare the behavior with that of the separate $LiCoO_2$ and graphite electrode (see Fig. 6a). As shown in Fig. 6b, the EIS was simulated using the equivalent circuit of Fig. 2c by Z-view software. It can be seen that the EIS of the 041428-type $LiCoO_2$/graphite batteries also fits the equivalent circuit of Fig. 2c. Table 4 shows the values of impedance parameters by simulating the EIS data of Fig. 6a. The R_{sei} and R_{ct} also decrease initially and then increase with the increase in the formation current. The value of R_{sei} is least using the formation protocol of c and the R_{ct} is least using the formation protocol of b. It can be found that the R_{ct} depends on the graphite anode, while the R_{sei} relies on the $LiCoO_2$ cathode. The lithium ion diffusion coefficient of $LiCoO_2$/graphite batteries decreases from formation protocol a to c and increases slightly from formation protocol c to d.

The best way to verify the effects of current on the formation $LiCoO_2$/graphite batteries is to test the cycling performance of batteries at different temperatures. It is seen

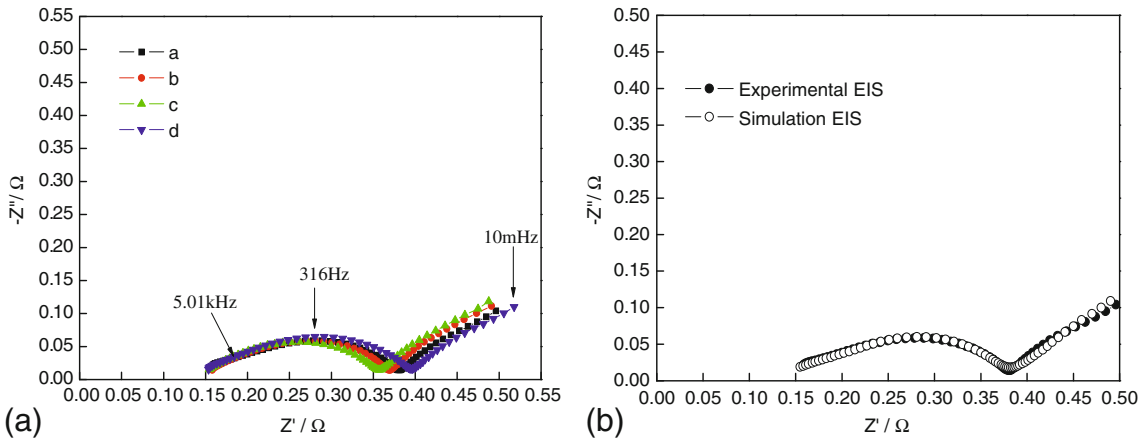

Fig. 6 EIS of 041428-type $LiCoO_2$/graphite batteries (**a**). Experimental and simulation EIS curves of *a* in **a** using the equivalent circuit of Fig. 2c by Z-view software (**b**)

Table 4 Impedance parameters of Fig.6a calculated using the equivalent circuit of Fig. 2c (the unit of R and CPE-T are Ω/cm^2 and F/cm^2, respectively)

Number	Rb	Rsei	Rct	CPE1		CPE2		Zw		
				T	P	T	P	R	T	P
a	6.14	4.09	5.56	0.00125	0.583	0.000604	0.748	16.37	25.96	0.507
b	6.10	4.05	4.32	0.00084	0.601	0.000601	0.830	17.91	28.33	0.516
c	5.94	3.28	4.75	0.00111	0.590	0.000606	0.796	19.34	29.80	0.502
d	5.94	3.82	5.91	0.00101	0.559	0.000645	0.768	17.99	29.34	0.499

in Fig. 7 that the batteries show best cycling performance using formation protocol b. With the increase or decrease in the formation current, the batteries show bad cycling performance, especially the high-temperature cycling performance. The bad cycling performance with a very low current may be due to the larger R_{cell} (composed of R_b, R_{sei}, and R_{ct}; see Fig. 6). The bad cycling performance using a big formation current may be attributed to two reasons: one is the larger R_{cell} and the other is the further reduction of the electrolytic solvents. It is well known that the SEI film on the anode with a high formation current is more loose (or porous) and less adhesive; the SEI with loose structure may not be sufficiently denser to prevent further electron tunneling. Therefore, the further reduction of the electrolytic solvents would still occur during battery cycling, which influences the cycling performance of batteries. However, Fig. 7a indicates that the formation current does not influence the cycling performance at 25 °C greatly, which indicates that the further reduction of the electrolytic solvents is not serious. Some of the SEI film with loose texture formed with a big formation current can be repaired and completed gradually during charge and discharge at low temperature. Whereas, Fig. 7b shows that the cycling performance of batteries at 50 °C is influenced greatly by the formation current. The reason may be that the SEI film with loose texture and poor adhesion formed with a large formation current cannot be repaired and completed during cycling at 50 °C, which leads to the bad cycling performance. However, the SEI film formed at low current is denser and stable at high temperature. The further reduction of the electrolytic solvents almost does not occur, which does not influence the performance of the battery obviously. The SEI film of graphite anode for $LiCoO_2$/graphite batteries is formed mainly below 3.6 V. Therefore, the lithium ion batteries should be activated using a proper current below 3.6 V to ensure a stable SEI film formed on the anode surface.

Conclusions

The activation characteristics and the effects of current densities on the formation of a separate $LiCoO_2$ and graphite electrode and the full $LiCoO_2$/graphite batteries have been studied. It was found that the EIS of the Li/graphite, $LiCoO_2$/Li, and $LiCoO_2$/graphite cells varied greatly with the increase of the formation current densities. The reduction reaction of electrolyte on the graphite anode surface occurred between 2.5 and 3.6 V to form a preliminary SEI film during the formation of the $LiCoO_2$/graphite batteries. The electrolyte was oxidized from 3.95 V vs Li^+/Li on the $LiCoO_2$ cathode surface to form a SEI film of cathode. However, the resistance of the SEI film formed on the $LiCoO_2$ electrode was much larger than that of the graphite anode. The $LiCoO_2$ cathode could be activated completely at the first cycle, while the activation

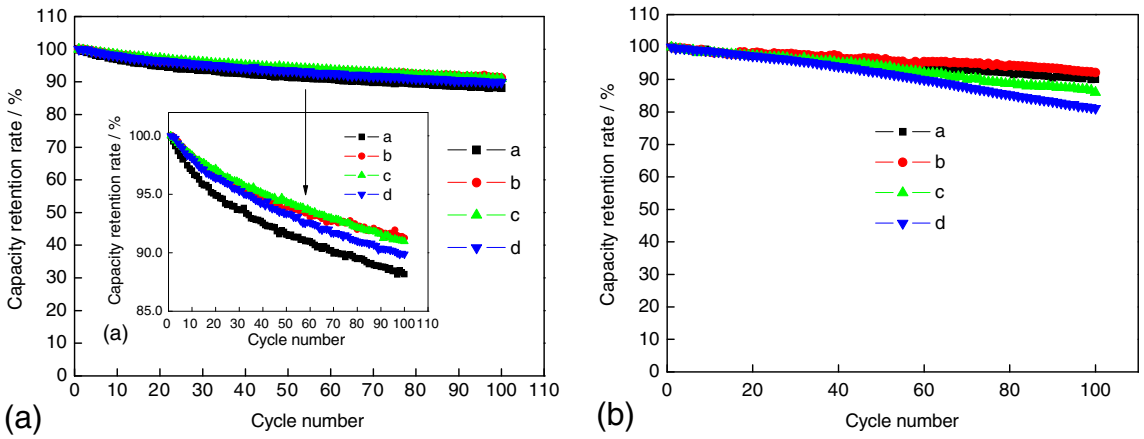

Fig. 7 Cycling performance of the 041428-type $LiCoO_2$/graphite batteries at different temperatures: **a** 25 °C; **b** 50 °C

of the graphite anode needed several cycles. The CE of the first cycle increased, but that of the second decreased with the increase in the formation current. The formation current influenced the high-temperature cycling performance obviously. Thus, the batteries should be activated with a proper current below 3.6 V to ensure an excellent formation of the SEI film formed on the anode surface.

Acknowledgments This work was supported by China Postdoctoral Science Foundation (no. 20100470296), Guangdong Province Energy and Environmental Materials Innovation R&D Team Plan and Dongguan McNair Technology Co., Ltd., China.

References

1. Itagaki M, Yotsuda S, Kobari N, Watanabe K, Kinoshita S, Ueb M (2006) Electrochim Acta 51:1629
2. Wang C, Appleby AJ, Little FE (2001) Electrochim Acta 46:1793
3. Zhang S, Shi P (2004) Electrochim Acta 49:1475
4. Zhang SS, Xu K, Jow TR (2004) Electrochim Acta 49:1057
5. Lee H-H, Wang Y-Y, Wan C-C, Yang M-H, Wu H-C, Shieh D-T (2004) J Power Sources 134:118
6. Jiang J, Dahn JR (2004) Electrochim Acta 49:4599
7. Matsui M, Dokko K, Kanamura K (2008) J Power Sources 177:184
8. Lee S-B, Pyun S-I (2002) Carbon 40:2333
9. Zhang SS, Xu K, Jow TR (2004) J Power Sources 130:281
10. Dedryvère R, Martinez H, Leroy S, Lemordant D, Bonhomme F, Biensan P, Gonbeau D (2007) J Power Sources 174:462
11. Zhang SS, Xu K, Jow TR (2006) Electrochim Acta 51:1636
12. He Y-B, Tang Z-Y, Song Q-S, Xie H, Liu Y-G, Xu Q (2008) J Electrochem Soc 155:A481
13. Peleda E, Golodnitsky D, Ulusa A, Yufita V (2004) Electrochim Acta 50:391
14. Nobili F, Tossici R, Croce F, Scrosati B, Marassi R (2001) J Power Sources 94:238
15. Croce F, Nobili F, Deptula A, Lada W, Tossici R, D'Epifanio A, Scrosati B, Marassi R (1999) Electrochem Commun 1:605
16. Umeda M, Dokko K, Fujita Y, Mohamedi M, Uchida I, Selman JR (2001) Electrochim Acta 47:885
17. Fey GTK, Yo WH, Chang YC (2002) J Power Sources 105:82
18. Itagaki M, Kobari N, Yotsuda S, Watanabe K, Kinoshita S, Ue M (2005) J Power Sources 148:78
19. Zhang SS, Xu K, Jow TR (2002) J Electrochem Soc 149:A1521